

# Evaluation of $^{64}\text{Cu}$ -DOTA- and $^{64}\text{Cu}$ -CBTE2A-Galectin-3 Peptide as a PET Radiotracer for Breast Carcinoma

Senthil R. Kumar<sup>1,2</sup>, Susan L. Deutscher<sup>1,2</sup>

<sup>1</sup>Department of Biochemistry, University of Missouri-Columbia School of Medicine, Columbia, MO 65211, USA

<sup>2</sup>Research Division, Harry S. Truman Veterans Hospital, Columbia MO 65201, USA

E-mail: [kumars@missouri.edu](mailto:kumars@missouri.edu), [deutschers@missouri.edu](mailto:deutschers@missouri.edu)

Received March 3, 2011; Revised April 3, 2011; Accepted April 30, 2011

## Abstract

Galectin-3 (Gal-3) is a  $\beta$ -galactosidase binding protein that modulates various cellular processes including cell adhesion, and metastasis. We evaluated the tumor targeting and imaging properties of a galectin-3 binding peptide originally selected from bacteriophage display, in a mouse model of human breast carcinoma expressing galectin-3. A galectin-3 binding peptide, ANTPCGPYTHDCPVKR, was synthesized with a Gly-Ser-Gly (GSG) spacer and 1,4,7,10, tetraazacyclododecane-N,N',N'',N'''-tetracetic acid (DOTA) or 4,11-bis(carboxymethyl)-1,4,8,11 tetrazabicyclo[6.6.2]hexadecane 4,11-diacetic acid (CB-TE2A), and radiolabeled with  $^{64}\text{Cu}$ . The synthesized peptides  $^{64}\text{Cu}$ -DO3A-(GSG)-ANTPCGPYTHDCPVKR ( $^{64}\text{Cu}$ -DO3A-pep) and  $^{64}\text{Cu}$ -CB-TE2A-(GSG)-ANTPCGPYTHDCPVKR ( $^{64}\text{Cu}$ -CB-TE2A-pep) demonstrated an  $\text{IC}_{50}$  value of  $(97 \pm 6.7)$  nM and  $(130 \pm 10.2)$  nM, respectively, to cultured MDA-MB-435 breast carcinoma cells *in vitro* in a competitive displacement binding study. The tumor tissue uptake in SCID mice bearing MDA-MB-435 tumors was  $(1.2 \pm 0.18)$  %ID/g ( $^{64}\text{Cu}$ -DO3A-pep) and  $(0.85 \pm 0.0.9)$  %ID/g ( $^{64}\text{Cu}$ -CB-TE2A-pep) at 30 min, respectively. While liver retention was moderate with both radiolabeled peptides the kidney retention was observed to be high. Radiation dose delivered to the tumor was estimated to be 42 mGy/mCi and 129 mGy/mCi with CB-TE2A and DO3A peptides, respectively. Imaging studies demonstrated tumor uptake with both  $^{64}\text{Cu}$ -DO3A- and  $^{64}\text{Cu}$ -CB-TE2A-(GSG)-ANTPCGPYTHDCPVKR after 2 h post injection. These studies suggest that gal-3 binding peptide could be developed into a PET imaging agent for galectin-3-expressing breast tumors.

**Keywords:** Galectin-3, Breast Cancer, PET Imaging, Peptide, Radiotracer

## 1. Introduction

Galectin-3 (Gal-3) is a 31 kDa protein, which has high affinity for  $\beta$ -galactosides, and possesses a highly conserved carbohydrate recognition domain (CRD) [1]. Gal-3 is found in the cytoplasm, but depending on cell types and proliferative states, it can also be detected on the cell surface [2], within the nucleus [3], and in the extracellular compartment [4,5]. Through its interaction with specific ligands, gal-3 is involved in multiple biological processes such as adhesion, apoptosis, inflammation, and metastasis [1,6,7]. Gal-3 has been found to be upregulated in a variety of human cancers including breast carcinoma [8]. Metastatic breast carcinoma cells express higher levels of gal-3 and have significantly increased adhesion to monolayers of endothelial cells compared with their non-metastatic counterparts [4].

One of the key steps in the initiation of metastasis is surface adhesion between tumor cells and endothelial cells [9,10]. Previous studies from our laboratory demonstrated that gal-3 is involved in heterotypic (carcinoma-endothelial cells) and homotypic (carcinoma-carcinoma) cellular adhesion via interactions with the tumor-specific Thomsen-Friedenreich (TF) mucin-type disaccharide, Gal 1-3GalNAc, expressed on most human adenocarcinomas [11]. Further, TF acts as a ligand for gal-3, and facilitates the mobilization of gal-3 to the surface of endothelial cells [11,12]. Thus, gal-3-carbohydrate interactions are crucial in cancer cell adhesion to the endothelium. Carbohydrate-based inhibitors that block gal-3-TF interactions [13,14], via binding to the CRD of gal-3 have previously been reported. However, such inhibitors bound other galectin family members due to their conserved carbohydrate binding residues which

undermine specificity [13]. We hypothesized that short synthetic peptides which bind to unique regions of the CRD of gal-3 with high specificity and affinity, may represent an alternative approach for targeting gal-3 on carcinoma cells.

Further, gal-3 molecules cluster at sites of cancer cell interaction and could be a potential target for cancer imaging and/or therapy [15]. Previously, we reported the selection of a gal-3 binding peptide ANTPCGPYTHDCPVKR (G3-C12) by combinatorial bacteriophage (phage) display techniques [16]. We also demonstrated successful imaging of human breast tumors expressing gal-3 with  $^{111}\text{In}$ -radiolabeled 1,4,7,10-tetrazacyclododecane-1,4,7,10-tetraacetic acid (DO3A)-(GSG)-G3-C12 [17] by single photon emission computed tomography (SPECT) in a mouse model. However, alternate imaging modalities have emerged in clinical medicine to generate high resolution images non-invasively. One such modality is positron emission tomography (PET), which utilizes the delivery of a pharmacologically significant molecule containing a positron-emitting radionuclide (e.g.  $^{64}\text{Cu}$  (half-life  $[t_{1/2}] = 12.7$  h) to a tissue or organ of interest [18].

The bifunctional chelator DOTA has been used for chelating  $^{64}\text{Cu}$ , however, its ability to chelate many +2 and +3 metal ions, and its relative instability compared to other chelators such as CB-TE2A, have made it less favourable [19,20]. CB-TE2A has been reported to form very stable complexes with  $^{64}\text{Cu}$  with less transchelation of the metal *in vivo* [21]. In the present study, we compared both  $^{64}\text{Cu}$ -DO3A-GSG-G3-C12 ( $^{64}\text{Cu}$ -DO3A-peptide) and  $^{64}\text{Cu}$ -CB-TE2A-GSG-G3-C12 ( $^{64}\text{Cu}$ -CB-TE2A-peptide) to evaluate the biodistribution and PET imaging properties of the peptides in a mouse model of human breast carcinoma.

## 2. Materials and Methods

### 2.1. Chemicals and Reagents

Amino acids and resin were purchased from Advanced Chem Tech (Louisville, KY). The bifunctional chelator CB-TE2A was synthesized as previously described [22]. DOTA was purchased from Macrocyclics (Richardson, TX). Copper-64 was purchased from Nuclear Reactor Laboratory, University of Wisconsin (Madison, WI). All other reagents in this study were obtained from Fisher Scientific Company (Pittsburgh, PA) unless otherwise specified.

### 2.2. Cell Lines

Human breast carcinoma cell line MDA-MB-435 and the normal mammary epithelial cell line 184A-1 were ob-

tained from American Type Tissue Culture. The MDA-MB-435 cells were maintained as monolayer cultures in RPMI-1640 medium supplemented with 10% FBS, sodium pyruvate, non-essential amino acids, and L-glutamine. The 184A-1 cells were grown in human mammary epithelial cell media (HuMEC) media supplemented with bovine pituitary extract. Cell cultures were maintained at 37°C in a 5% CO<sub>2</sub> humidified incubator.

### 2.3. Peptide Synthesis

Solid phase synthesis of DO3A- and CB-TE2A-G3-C12 peptide (ANTPCGPYTHDCPVKR) with a Gly-Ser-Gly (GSG) amino acid spacer between the chelator and amino terminus of the peptide was carried out using an Advanced ChemTech 396 multiple peptide synthesizer (Advanced Chem Tech, Louisville, KY). The chelator CB-TE2A was coupled to the amino terminus of the linear GSG-G3-C12 through an intermediate preparation of the activated mixed anhydride by use of DIC/DIEA/DMF as described earlier [22]. Reverse phase high pressure liquid chromatography (RP-HPLC) analysis of synthesized peptides was performed using a C18 column (218TP54; Vydac, Hesperia, CA). The mobile phase consisted of a linear gradient system, with solvent A corresponding to 100% water with 0.1% trifluoroacetic acid (TFA) and solvent B corresponding to 100% acetonitrile with 0.1% TFA. Identities of the peptides were confirmed by electrospray ionization mass spectrometry (ESI-MS) (Mass Consortium Corporation, San Diego, CA).

### 2.4. Radiolabeling of DO3A- and CB-TE2A-(GSG)-G3-C12 Peptide

Radiolabeling CB-TE2A-(GSG)-G3-C12 peptide with  $^{64}\text{Cu}$  was performed as follows. CB-TE2A-(GSG)-G3-C12 (30 µg) was radiolabeled with ~ 30.0 MBq (810 µCi)  $^{64}\text{Cu}$  in ammonium acetate (0.4 M) pH 7.0, at 80°C for 60 min. The reaction buffer was purged extensively with nitrogen prior to radiolabeling in order to minimize peptide oxidation, and contained Tris-(2-carboxyethyl) phosphine hydrochloride (TCEP) in order to prevent disulfide bond formation between cysteines. The resulting radiolabeled peptide conjugates were peak purified using a Phenomenex (Torrence, CA) Jupiter 5u C18 300 Å 250 × 4.6 mm columns and RP-HPLC (10% - 95% acetonitrile/0.1% TFA) for 30 min in order to separate the radiolabeled peptide from their nonradiolabeled counterparts. For concentrating, the peak-purified peptides were percolated through Empore high efficiency (C18) extraction disk cartridges (St. Paul, MN), and eluted with 400 µl of an 8:2 ethanol/sterile saline solution. The ethanol was evaporated under a stream of nitrogen and was diluted to

the appropriate volume with sterile saline. Radiochemical yields for  $^{64}\text{Cu}$ -DO3A-peptide and  $^{64}\text{Cu}$ -CB-TE2A-peptide averaged 45% and 40%, respectively. Radiochemical purity of both  $^{64}\text{Cu}$ -labeled peptides was found to be  $\geq 98\%$  pure.

For non-radioactive Cu-labeling, 0.5 mg samples of DO3A- or CB-TE2A-peptide were dissolved in 500  $\mu\text{L}$  of ammonium acetate buffer (as described previously for DO3A and CB-TE2A)/0.8 mM copper(II) sulfate-pentahydrate solution. The solutions were heated at identical conditions as mentioned above for radiolabeling, and allowed to cool to room temperature. Native copper ( $^{\text{nat}}\text{Cu}$ )-peptides were then peak purified by RP-HPLC and determined to be  $\geq 97\%$  pure. ESI-MS was performed to check the integrity of the peptides.

## 2.5. Cell Binding Assay

Approximately  $1.0 \times 10^6$  of MDA-MB-435 or 184A-1 cells/tube were incubated at  $37^\circ\text{C}$  for different time intervals (10, 30, 45, 60, 90 and 120 min) with  $1 \times 10^5$  cpm  $^{64}\text{Cu}$ -DO3A- or  $^{64}\text{Cu}$ -CB-TE2A-peptide in 0.3 mL of cell binding media (RPMI 1640 with 25 mM HEPES, pH 7.4, 0.2% BSA, 3 mM 1,10-phenanthroline). At different time points, the cells were pelleted by centrifugation and washed twice with ice-cold 0.01 M PBS, pH 7.4, 0.2% BSA. After removing the supernatant by centrifugation, the radioactivity associated with the cells was quantitated in a Wallac  $\gamma$  counter (PerkinElmer Life and Analytical Sciences Inc., Waltham, MA). Cell binding ability was reported as total radioactivity (cpm) that was bound to the cells.

## 2.6. In Vitro Competitive Cell Binding Affinity and Serum Stability Studies

A competitive displacement binding assay was used to determine the fifty-percent inhibitory concentration ( $\text{IC}_{50}$ ) for radiolabeled G3-C12 peptide using  $^{\text{nat}}\text{Cu}$ -DO3A- or  $^{\text{nat}}\text{Cu}$ -CB-TE2A-peptide as the displacement ligand. Approximately,  $2.0 \times 10^6$  MDA-MB-435 cells/tube were suspended in cell binding media along with  $2.5 \times 10^4$  cpm of each  $^{64}\text{Cu}$ -DO3A or  $^{64}\text{Cu}$ -CB-TE2A-peptide and a range of concentrations ( $10^{-5}$  -  $10^{-12}$  M) of respective non-radiolabeled counterparts and incubated at  $37^\circ\text{C}$  for 60 min. The supernatant was removed after pelleting the cells by centrifugation. The cell pellet was further washed twice with 0.5 mL of ice-cold binding buffer. Cell-associated radioactivity was measured in a  $\gamma$  counter and the binding affinity was determined using Graft software (Erithacus Software Limited, Surrey, UK).

*In vitro* serum stability of the radiolabeled peptide conjugates was tested by incubating 30.0 MBq (810  $\mu\text{Ci}$ )

of  $^{64}\text{Cu}$ -DO3A- or  $^{64}\text{Cu}$ -CB-TE2A-peptide in 0.3 mL of mouse serum at  $37^\circ\text{C}$  for 0.5, 1, 2, 4 and 24 h, respectively. At various time points, 30  $\mu\text{L}$  were removed and the proteins precipitated with 30  $\mu\text{L}$  acetonitrile. The samples were centrifuged at 12,500 rpm for 5 min and the cleared lysate ( $\sim 25$   $\mu\text{L}$  aliquots) was analyzed by RP-HPLC with a 0% - 95% gradient acetonitrile in 30 min to assess the integrity of the radioconjugates.

## 2.7. Pharmacokinetic Studies in Mice Bearing Human Breast Tumors

All animal studies were conducted in accordance with highest standards of care according to the National Institute of Health guide for care and use of laboratory animals and the policy and procedure for animal research at the Harry S. Truman Veterans Hospital. Female 4 - 6 week old SCID (ICR-SCID) mice were obtained from Taconic (Hudson, NY). The mice were implanted subcutaneously in the right shoulder with  $1 \times 10^7$  MDA-MB-435 human breast carcinoma cells. Fully grown tumors ranged from 0.28 - 0.85 g (3 - 4 wk after inoculation). Each mouse (three mice per time point) was injected in the tail vein with 0.185 MBq (5  $\mu\text{Ci}$ ) of  $^{64}\text{Cu}$ -DO3A- or  $^{64}\text{Cu}$ -CB-TE2A-peptide in 100  $\mu\text{L}$  saline. The mice were sacrificed by cervical dislocation and their tissues and organs excised at different time points (30 min, 1, 2, 4, and 24 h) post injection (p.i.). The excised tissues were weighed, and the tissue activity was measured in a  $\gamma$  counter. The percent injected dose (%ID) and percent injected dose per gram (%ID/g) were determined for each tissue. Whole blood %ID and %ID/g were determined assuming the blood accounted for 6.5% of the body weight of the mouse. Tumor blocking studies was performed by administering  $^{\text{nat}}\text{Cu}$ -DO3A- or  $^{\text{nat}}\text{Cu}$ -CB-TE2A-peptide (120  $\mu\text{g}$ ) in MDA-MB-435 tumor mice ( $n = 3$ ) 20 min before administering respective radiolabeled counterparts. After 2 h, a biodistribution study were performed as describe above and %ID/g was determined for each tissue.

Inhibition experiments with bovine serum albumin fragments (BSA-f) were performed to reduce the kidney retention of the radiolabeled peptides during biodistribution studies [23]. Briefly, 3.0 g of BSA in 50 mM ammonium carbonate (15 mL) was subjected to trypsin (335 mg) digestion at  $37^\circ\text{C}$  for 24 h. The trypsin-digested sample was filtered using 50 kDa Centriprep (YM-50) centrifugal filters (Millipore, Billerica, MA). The filtrate containing albumin fragments  $< 50$  kDa, was further fractionated using an YM-3 filter (3 kDa cutoff) which yielded albumin fragments  $< 3$  kDa (filtrate), and fragments with molecular weight range of 3 - 50 kDa (residue). The 3 - 50 kDa albumin fragment(s) (200 g) sample in normal saline (100  $\mu\text{L}$ ) was pre-injected into the

MDA-MB-435 tumor bearing mice ( $n = 3$ ) via the tail vein. After 5 min, 0.185 MBq (5  $\mu$ Ci) of  $^{64}\text{Cu}$ -DO3A- or  $^{64}\text{Cu}$ -CB-TE2A-peptide was administered into the mice. The mice were sacrificed after 2 h, and the kidney uptake of the radiolabeled peptides was measured in a  $\gamma$ -counter. Control experiments ( $n = 3$ ) were run in parallel with pre-injection of normal saline instead of albumin fragments.

## 2.8. Dosimetry Studies

The biodistribution data was processed with a dosimetry model to determine doses to all organs and to the tumor in the mouse model. The dosimetry model being used is a derivation on that developed by Hui *et al.* [24] to provide realistic beta dose estimates for organs in mice that received therapeutic radiopharmaceuticals for high energy betas. This model is required because the beta range of candidate radioisotopes such as  $^{64}\text{Cu}$  is large relative to the size of many of the organs. This model has already been used to calculate the necessary dosimetry values for several isotopes including  $^{64}\text{Cu}$  [25].

## 2.9. MicroPET/MicroCT Studies

*In vivo* microPET/CT of MDA-MB-435 tumor-bearing mice with  $^{64}\text{Cu}$ -DO3A- or  $^{64}\text{Cu}$ -CB-peptides were performed. Tissue data imaging analysis was performed on a MDA-MB-435 tumor bearing mice in a microPET scanner 2 h after intravenous injection of 12.0 MBq (324  $\mu$ Ci) of the radiolabeled peptides in a small animal PET scanner (MOSAIC small animal PET unit (Philips, USA)). This PET scanner has a transverse field of view (FOV) of 12.8 cm and a gantry diameter of 21 cm, and operates in a 3-dimensional mode (3D). The mouse to be imaged was laser aligned at the center of the scanner FOV for imaging. The microPET image reconstruction was performed with a 3D row-action maximum-likelihood algorithm (RAMLA). The microCT was performed for the purpose of anatomic/molecular data fusion, and concurrent image reconstruction was performed with a Fanbeam (Feldkamp) filtered-backprojection algorithm. Reconstructed DICOM (Digital Imaging and Communication in Medicine) PET images were imported into AMIRA 3.1 software (Visage Imaging, Inc. San Diego, CA) for subsequent image fusion with microCT and 3D visualization.

## 2.10. Statistical Analysis

Data are expressed as mean  $\pm$  SD. Mean values were compared using the Student's *t* test. Differences were considered statistically significant for  $P \leq 0.05$ .

## 3. Results and Discussion

The DO3A- and CB-TE2A-peptides was prepared by solid-phase peptide synthesis using standard F-moc procedures [26]. In order to enhance the conformational freedom, a GSG spacer was introduced between the chelators and the amino-terminus of the peptides [24].  $^{nat}\text{Cu}$ -labeled peptides was prepared by heating aqueous solutions of the peptides with  $\text{CuSO}_4 \cdot 5\text{H}_2\text{O}$  at  $85^\circ\text{C}$  for 60 min.  $^{nat}\text{Cu}$ -labeled peptides were purified and analyzed by mass spectrometry before cell binding assays. The calculated and observed molecular weights of the  $^{nat}\text{Cu}$ -peptides were 2405.0 Da and 2405.3 Da (DO3A-peptide) and 2342.0 and 2342.5 Da (CB-TE2A-peptide), respectively. For radiolabeling, the peptides were labeled with  $^{64}\text{Cu}$  in ammonium acetate buffer (pH 7.0) at  $85^\circ\text{C}$  for 1 h, and further purified by RP-HPLC in order to separate the radiolabeled peptides from their non-radiolabeled counterparts.  $^{64}\text{Cu}$ -DO3A- and  $^{64}\text{Cu}$ -CB-TE2A-peptide eluted with a retention time ( $t_r$ ) of 13.2 min and 13.8 min, respectively, a minute after the elution of their respective non-radiolabeled counterparts. The radiolabeled peptides were obtained at a purity of  $\geq 98\%$ .

Specific binding of radiolabeled peptides was demonstrated with MDA-MB-435 cells. Minimal or no binding was observed with 184A-1 control cells. The time course experiments (**Figure 1**) revealed the association of radiolabeled peptide with the MDA-MB-435 cells which increased gradually and equilibrium was reached at 1 h, beyond which no further increase in cell associated radioactivity was observed. Total cell binding capacity was  $\sim 1\%$  compared to the initial total radioactivity added to breast carcinoma cells. MDA-MB-435 human breast carcinoma cells were originally derived from a pleural effusion of a woman with metastatic ductal breast carcinoma [27]. However, there has been speculation that the original MDA-MB-435 cancer cells were lost early after their establishment and found to be identical with the M-14 melanoma cell line [28]. On the contrary, a recent report revealed that both MDA-MB-435 and M-14 are of MDA-MB-435 breast cancer origin [29]. Despite these speculations, the MDA-MB-435 cell line has been widely used as a breast carcinoma model and remains one of the most reliable *in vivo* models of human breast cancer.

Competitive binding displacement assays in MDA-MB-435 cells were performed using various concentrations ( $10^{-5}$  to  $10^{-12}$  M) of  $^{nat}\text{Cu}$ -DO3A- or  $^{nat}\text{Cu}$ -CB-TE2A-peptide as the displacement radioligand. Decrease in bound radioactivity to the cultured MDA-MB-435 cells was observed with increasing concentration of respective non-radiolabeled peptide (**Figure 2**). Data analysis indicated that the  $\text{IC}_{50}$  value for the radiolabeled

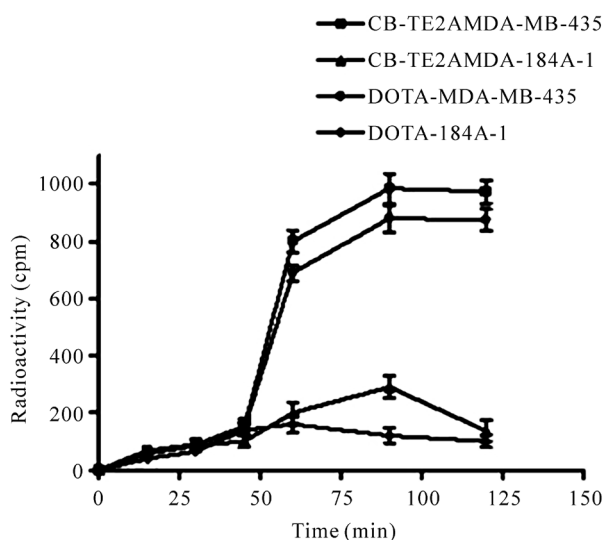


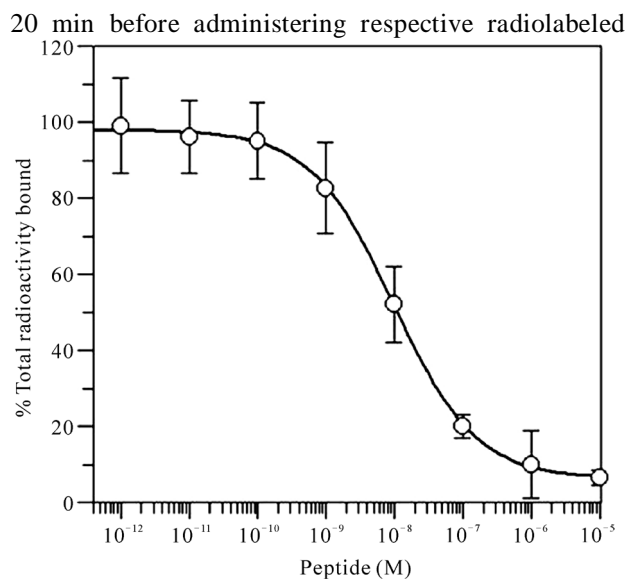
**Figure 1.** The gal-3 binding properties of the radiolabeled  $^{64}\text{Cu}$ -DO3A-peptide and  $^{64}\text{Cu}$ -CB-TE2A-peptide. Approximately,  $1.0 \times 10^6$  cells/tube were incubated at  $37^\circ\text{C}$  for different time intervals with  $1.0 \times 10^5$  cpm radioligand. While the radiolabeled peptide demonstrated binding to human MDA-MB-435 breast carcinoma cells, minimal binding was observed with normal mammary epithelial (184A1) cells.

peptides was  $(97 \pm 6.7)$  nM (DO3A-peptide) and  $(130 \pm 10.0)$  nM (CB-TE2A-peptide), respectively.

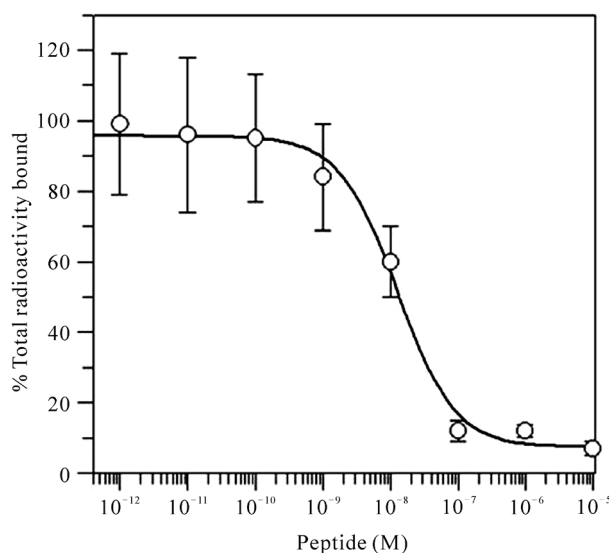
This affinity was found to be slightly higher than what has been reported previously for  $^{111}\text{In}$ -DO3A-(GSG)-G3-C12 ( $(200.0 \pm 6.7)$  nM) [17]. The affinity values were also in keeping with that of G3-C12 ( $88 \pm 23.0$  nM) toward recombinant gal-3 protein, as determined by fluorescent titration experiments [16].

The metabolic stability of the  $^{64}\text{Cu}$ -labeled peptides in serum was analyzed at different time points at  $37^\circ\text{C}$  by RP-HPLC. Both the peptides were stable in serum for periods up to 4 h. However, at 24 h an additional peak was observed with both radiolabeled peptides prior to the original radiolabeled peptide peak suggesting the degradation of peptides during prolonged serum incubation. A representative RP-HPLC profile of  $^{64}\text{Cu}$ -CB-TE2A-peptide is shown in **Figure 3**. A similar profile was observed with  $^{64}\text{Cu}$ -DO3A-peptide.

Detailed *in vivo* studies in SCID mice bearing human MDA-MB-435 tumor xenografts at different time intervals indicated  $^{64}\text{Cu}$ -DO3A-peptide tumor accumulation of  $(1.2 \pm 0.18)$  %ID/g,  $(0.7 \pm 0.16)$  %ID/g,  $(0.61 \pm 0.04)$  %ID/g, and  $(0.59 \pm 0.03)$  %ID/g; and CB-TE2A-peptide,  $(0.85 \pm 0.62)$  %ID/g,  $(0.72 \pm 0.17)$  %ID/g,  $(0.68 \pm 0.07)$  %ID/g and  $(0.19 \pm 0.03)$  %ID/g in tumor tissue at 30 min, 1 h, 2 h, and 4 h, respectively (**Tables 1** and **2**). For tumor blocking studies,  $^{\text{nat}}\text{Cu}$ -DO3A- or  $^{\text{nat}}\text{Cu}$ -CB-TE2A-peptide ( $120 \mu\text{g}$ ) was administered in MDA-MB-435 tumor mice ( $n = 3$ )



(a)



(b)

**Figure 2.** Competitive binding assays using MDA-MB-435 cells. Displacement of (a)  $^{64}\text{Cu}$ -DO3A-peptide and (b)  $^{64}\text{Cu}$ -CB-TE2A-peptide by respective  $^{\text{nat}}\text{Cu}$ -peptide counterpart is shown. MDA-MB-435 cells ( $2 \times 10^6$ /tube) were incubated with  $2.5 \times 10^4$  cpm radioligand and increasing concentrations of the  $^{\text{nat}}\text{Cu}$ -peptide. Each data point represents the mean  $\pm$  SD of three replicates.  $\text{IC}_{50}$  value obtained was  $(97 \pm 6.7)$  nM ( $^{64}\text{Cu}$ -CB-TE2A-peptide), respectively.

counterparts. This approach reduced  $\sim 43\%$  and  $\sim 47\%$  of tumor uptake of the radiolabeled peptides (**Tables 1** and **2**) compared to mice injected with radioactive peptide alone ( $P = 0.03$ ). Overall, the radiolabeled peptide conjugate showed fast whole body clearance from the mouse. The observed partial blocking upon injection of the non-radiolabeled peptide could be due to faster

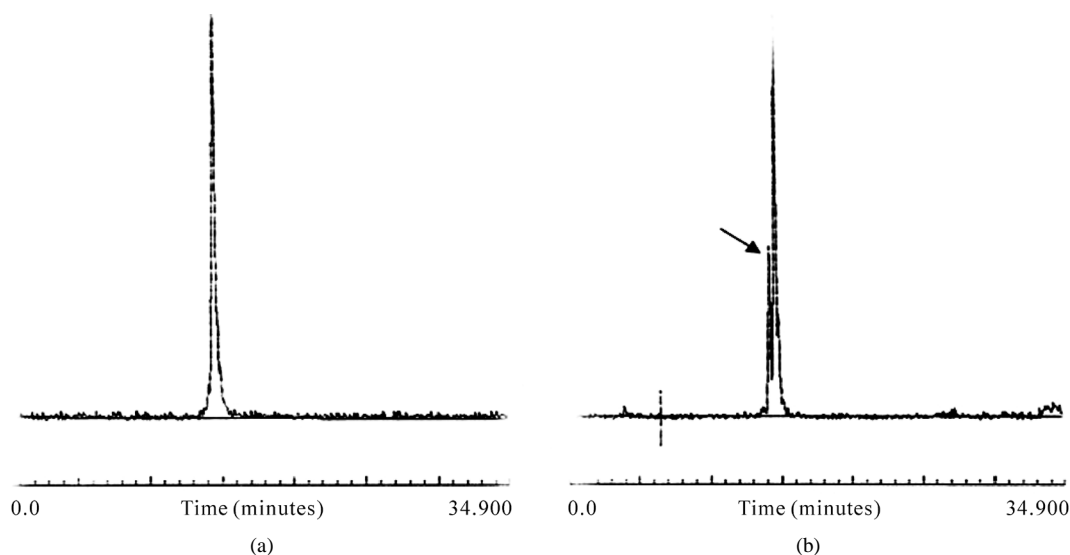


**Figure 3.** The serum stability of  $^{64}\text{Cu}$ -CB-TE2A-peptide at 0 and 24 h. (a) Elution of  $^{64}\text{Cu}$ -CB-TE2A-peptide at 0 time point. (b) At 24 h, an additional peptide peak (arrow) was observed prior to the original radiolabeled peptide suggesting the degradation of peptide during prolonged serum incubation.

**Table 1.** Biodistribution studies of  $^{64}\text{Cu}$ -DO3A-peptide using MDA-MB-435 tumor bearing SCID mice.

Tissues	0.5 h	1 h	2 h	2 h block	4 h	24 h
<b>Percent injected dose/gram (%ID/g)<sup>a</sup></b>						
Tumor	1.20 ± 0.18	0.70 ± 0.16	0.61 ± 0.04	0.35 ± 0.07 <sup>b</sup>	0.59 ± 0.04	0.22 ± 0.12
Blood	1.59 ± 0.24	0.47 ± 0.05	0.28 ± 0.08	0.25 ± 0.05	0.17 ± 0.05	0.15 ± 0.02
Brain	0.05 ± 0.01	0.04 ± 0.01	0.03 ± 0.01	0.02 ± 0.00	0.05 ± 0.01	0.01 ± 0.00
Heart	0.64 ± 0.09	0.36 ± 0.01	0.36 ± 0.02	0.29 ± 0.07	0.12 ± 0.03	0.08 ± 0.01
Lung	1.25 ± 0.07	0.89 ± 0.23	0.78 ± 0.11	0.75 ± 0.10	0.27 ± 0.20	0.19 ± 0.12
Liver	1.78 ± 0.16	2.41 ± 0.36	2.40 ± 0.14	2.30 ± 0.17	1.43 ± 0.21	0.95 ± 0.11
Spleen	0.51 ± 0.04	0.40 ± 0.21	0.55 ± 0.10	0.57 ± 0.20	0.23 ± 0.15	0.13 ± 0.02
Stomach	0.52 ± 0.17	0.59 ± 0.07	0.63 ± 0.04	0.69 ± 0.00	0.17 ± 0.05	0.10 ± 0.02
Kidneys	85.31 ± 10.63	96.0 ± 6.70	75.3 ± 5.88	79.2 ± 3.57	77.13 ± 8.26	18.2 ± 4.40
Muscle	0.29 ± 0.06	0.11 ± 0.01	0.07 ± 0.00	0.05 ± 0.02	0.05 ± 0.00	0.01 ± 0.00
Pancreas	0.41 ± 0.11	0.23 ± 0.08	0.22 ± 0.07	0.19 ± 0.02	0.12 ± 0.01	0.06 ± 0.00
Bone	0.28 ± 0.04	0.19 ± 0.07	0.11 ± 0.03	0.09 ± 0.01	0.09 ± 0.02	0.03 ± 0.01
<b>Percent injected dose (%ID)</b>						
Intestines	1.54 ± 0.08	1.65 ± 0.14	2.20 ± 0.30	2.09 ± 0.46	3.48 ± 0.47	2.70 ± 0.70
Urine	55.22 ± 8.70	64.5 ± 1.60	69.8 ± 3.10	77.41 ± 4.80	66.4 ± 3.70	84.4 ± 4.0
<b>Uptake ratio of tumor/normal tissue</b>						
Tumor/blood	0.75	1.50	2.18	---	3.47	1.46
Tumor/Muscle	4.13	4.27	8.70		11.8	22.0
Tumor/liver	0.67	0.29	0.25		0.41	0.23

<sup>a</sup>Data are presented as %ID/g ± SD except for intestines and urine, values for which are expressed as %ID/g ± SD (n = 3); <sup>b</sup>P = 0.03, significance comparison between the tumor uptake of radiolabeled peptide in the absence and presence of its non-radiolabeled counterpart at 2 h p.i.

**Table 2. Biodistribution studies of  $^{64}\text{Cu}$ -CB-TE2A-peptide using MDA-MB-435 tumor bearing SCID mice.**

Tissues	0.5 h	1 h	2 h	2 h block	4 h	24 h
<b>Percent injected dose/gram (%ID/g)<sup>a</sup></b>						
Tumor	0.85 ± 0.12	0.72 ± 0.10	0.68 ± 0.07	0.36 ± 0.08 <sup>b</sup>	0.25 ± 0.10	0.10 ± 0.01
Blood	1.57 ± 0.26	0.42 ± 0.15	0.07 ± 0.00	0.08 ± 0.03	0.06 ± 0.00	0.04 ± 0.01
Brain	0.05 ± 0.01	0.03 ± 0.01	0.01 ± 0.00	0.01 ± 0.00	0.01 ± 0.00	0.00 ± 0.00
Heart	0.56 ± 0.07	0.20 ± 0.10	0.06 ± 0.01	0.10 ± 0.04	0.08 ± 0.02	0.07 ± 0.01
Lung	1.33 ± 0.20	0.61 ± 0.12	0.29 ± 0.05	0.27 ± 0.08	0.25 ± 0.11	0.22 ± 0.05
Liver	1.34 ± 0.23	1.23 ± 0.30	0.97 ± 0.10	1.02 ± 0.21	1.21 ± 0.11	0.79 ± 0.07
Spleen	0.50 ± 0.11	0.35 ± 0.06	0.20 ± 0.04	0.19 ± 0.02	0.24 ± 0.11	0.15 ± 0.05
Stomach	0.44 ± 0.12	0.18 ± 0.06	0.15 ± 0.04	0.15 ± 0.01	0.17 ± 0.08	0.13 ± 0.06
Kidneys	91.5 ± 21.0	98.0 ± 24.2	83.31 ± 19.0	81.2 ± 7.20	82.0 ± 8.65	39.03 ± 3.0
Muscle	0.23 ± 0.02	0.08 ± 0.03	0.06 ± 0.01	0.02 ± 0.00	0.07 ± 0.04	0.05 ± 0.01
Pancreas	0.31 ± 0.10	0.14 ± 0.09	0.16 ± 0.05	0.14 ± 0.03	0.18 ± 0.09	0.17 ± 0.08
Bone	0.16 ± 0.09	0.12 ± 0.05	0.10 ± 0.08	0.12 ± 0.05	0.10 ± 0.02	0.03 ± 0.01
<b>Percent injected dose (%ID)</b>						
Intestines	1.54 ± 0.08	0.62 ± 0.12	0.69 ± 0.06	0.66 ± 0.08	0.90 ± 0.14	0.59 ± 0.23
Urine	51.3 ± 4.50	64.2 ± 8.20	73.2 ± 2.60	76.1 ± 4.90	70.6 ± 4.99	86.5 ± 0.70
<b>Uptake ration of tumor/normal tissue</b>						
Tumor/blood	0.54	1.71	9.70	----	4.2	2.5
Tumor/muscle	3.70	9.00	11.33		3.6	2.0
Tumor/liver	0.60	0.58	0.70		0.21	0.13

<sup>a</sup>Data are presented as %ID/g ± SD except for intestines and urine, values for which are expressed as %ID ± SD (n = 3); <sup>b</sup>P = 0.032, significance comparison between the tumor uptake of radiolabeled peptide in the absence and presence of its non-radiolabeled counterpart at 2 h p.i.

clearance of the competing peptide from circulation, and longer residence time of the competing molecule might aid in more efficient blocking of the radioligand. Whether increasing the dose of the non-radiolabeled peptide further could compete off the radiolabeled peptide binding to the tumor is not clear. In the future, a dose-ranging study with <sup>nat</sup>Cu-labeled peptides could shed some light on the blocking efficiency of this peptide.

The majority of the peptides in circulation cleared through the renal system (DO3A-peptide—(69.9 ± 3.1) %ID; CB-TE2A peptide—(73.3 ± 2.64) %ID) and less through the hepatobiliary system (DO3A-peptide—(2.45 ± 0.27) %ID; CB-TE2A peptide—(0.96 ± 0.06) %ID) at the end of 2 h. The disappearance of radiolabeled peptides from the blood was comparable between the two peptides, (1.59 ± 0.24) %ID/g (DO3A-peptide) and (1.57 ± 0.26) %ID/g (CB-TE2A-peptide) at 30 min p.i. However, at 2 h and beyond a rapid disappearance of CB-TE2A-peptide from blood was observed compared to DOTA-peptide (P = 0.015). Variable radiolabeled pep-

tide uptake was observed in normal tissues. Most of the tissues exhibited minimal uptake, while modest radioactivity was observed mainly in lungs and liver. Lung radioactivity with DO3A-peptide was higher at all time points beyond 1 h p.i., compared to CB-TE2A-peptide (P = 0.048). While the washout of radioactivity in the lungs with DO3A-peptide was not prominent, CB-TE2A-peptide disappearance was observed after 1 h time point. Radioactivity uptake in the liver for DO3A-peptide and CB-TE2A-peptide was similar at 30 min p.i., with values of (1.78 ± 0.16) %ID/g and (1.34 ± 0.23) %ID/g, respectively. However, at time points 1 h and later the DO3A-peptide accumulation in liver was higher than that of the CB-TE2A-peptide (P = 0.01). Copper radioisotopes have been shown to transchelate from the chelation systems such as 1,4, 7,10-tetra-azacyclododecane-N,N',N'', N'''-tetraacetic acid (DOTA) and 1,4,8,11-tetraazacyclotetradecane-, N,N',N'' N'''-tetraacetic acid (TETA) [30]. The transchelated metals bind to proteins in liver (e.g. superoxide dismutase) and to serum albumin [31]. Earlier

work by Weisman and coworkers suggested that CB-TE2A chelator can stabilize copper due to the rigidity of its crossbridge system which offers increased kinetic stability compared to DOTA or TETA, thereby reducing transchelation of  $^{64}\text{Cu}$  [30].

Previous studies indicated that the injection of  $[^{64}\text{Cu}]\text{Cu}^{2+}$  alone in mice, resulted in half the injected dose (~54%) concentrated in the liver after 2 h [32]. Moreover, oral administration of copper acetate in tumor bearing mice revealed the accumulation of copper in liver (~62.1  $\mu\text{g/g}$  tissue) and kidneys (~4.8  $\mu\text{g/g}$  tissue) [32]. Though we observed serum stability of the radiolabeled peptides *in vitro*, radioactivity in the liver suggests that transchelation of  $^{64}\text{Cu}$  could occur from the radiolabeled peptides, *in vivo*. Such a scenario was reported earlier for  $^{64}\text{Cu}$ -DOTA [30], and for  $^{64}\text{Cu}$ -TETA, where *in vitro* serum stability was high [33] while *in vivo* there was transchelation of  $^{64}\text{Cu}$  to superoxide dismutase and other proteins [31].

Substantial uptake in kidneys was observed at 2 h p.i., for  $^{64}\text{Cu}$ -DO3A-peptide ( $(75.32 \pm 5.88) \% \text{ID/g}$ ) and  $^{64}\text{Cu}$ -CB-TE2A-peptide ( $(83.31 \pm 19.0) \% \text{ID/g}$ ) which declined to  $(18.2 \pm 4.4) \text{ID/g}$  and  $(39.03 \pm 3.0) \% \text{ID/g}$  at the end of 24 h, respectively. This high renal uptake and slow excretion could be due to the overall charge of the peptide. Previous studies have reported the effect of peptide charge on kidney uptake of both  $^{64}\text{Cu}$  and  $^{111}\text{In}$ -labeled compounds [34,35]. Indium-111-DTPA-conjugated peptides are retained in the kidney after reabsorption by renal tubular cells and lysosomal proteolysis [34]. Renal retention of  $^{111}\text{In}$  activity was highest with positively charged and lowest for negatively charged particles, respectively [36]. Similar charge effects were also seen with  $^{64}\text{Cu}$ -labeled azamacrocycles [31]. Although studies including ours have reported that blocking the cationic binding sites in the kidney with D- or L-lysine [17,24,37] could decrease the peptide retention in the kidney, complete inhibition of uptake was not achievable.

The absorbed radiation doses to tumor and normal organs from the radiolabeled peptides were estimated in this study based on the biodistribution data in MDA-MB-435 human breast xenografted SCID mice (Table 3). Dosimetry calculations were based on energy deposition from the  $\beta$ -decay of  $^{64}\text{Cu}$ . The absorbed dose from CB-TE2A and DO3A peptide to the tumor was 42 mGy/mCi and 129 mGy/mCi, respectively. Normal tissue doses were low except for the kidneys, which were estimated at 16,281 mGy/mCi (CB-TE2A) and 7381 mGy/mCi (DO3A). These results suggest that the kidneys will be the dose-limiting normal organ.

In order to reduce the kidney uptake of the radiolabeled peptides, BSA-f (3 - 50 kDa) generated by tryptic

digestion was used as a blocking agent. The renal uptake of radiolabeled peptides without and with co-infusion of 200  $\mu\text{g}$  of BSA-f was performed in SCID mice ( $n = 3$

**Table 3. Absorbed radiation doses from radiolabeled peptides in MDA-MB-435 tumor bearing SCID mice.**

Organ	CB-TE2A-peptide	DO3A-peptide
Tumor	42	129
Blood	40	116
Brain	02	60
Heart	26	158
Lung	71	235
Liver	302	546
Spleen	49	156
Stomach	46	166
Kidneys	16,289	7381
Muscle	04	15
Pancreas	38	110
Bone	27	29

Dosimetry calculations were based on energy deposition from the  $\beta$ -decay of  $^{64}\text{Cu}$ . The values are given in mGy/mCi.

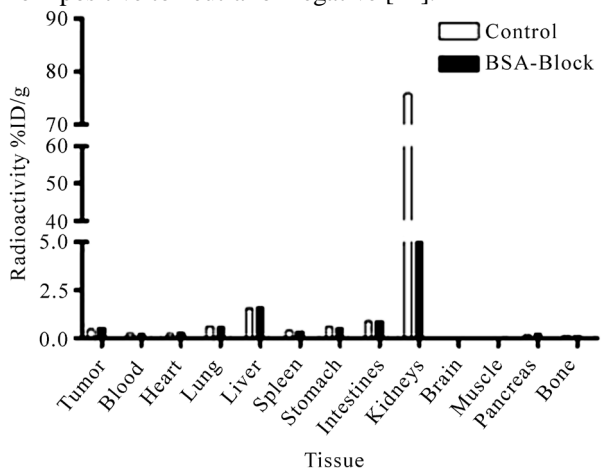
each) (Figure 4). Results indicated a ~43% ( $^{64}\text{Cu}$ -DO3A-peptide,  $P = 0.032$ ) and ~47% ( $^{64}\text{Cu}$ -CB-TE2A-peptide,  $P = 0.037$ ) inhibition of renal radioligand uptake compared to the radiotracer only group. However, no notable difference in the uptake of radioligand in other tissues and organs was observed.

MicroPET imaging studies of  $^{64}\text{Cu}$ -DO3A- or CB-TE2A-peptide in MDA-MB-435 tumor bearing mice at 2 h p.i., demonstrated their use as a PET targeting agent for primary breast tumors. Fused microPET/CT of MDA-MB-435 tumor-bearing SCID mice at 2 h p.i., are shown in Fig 5. In order to better visualize the tumor uptake of the radiolabeled peptides along with reduced background, the imaging was performed at 2 h p.i.

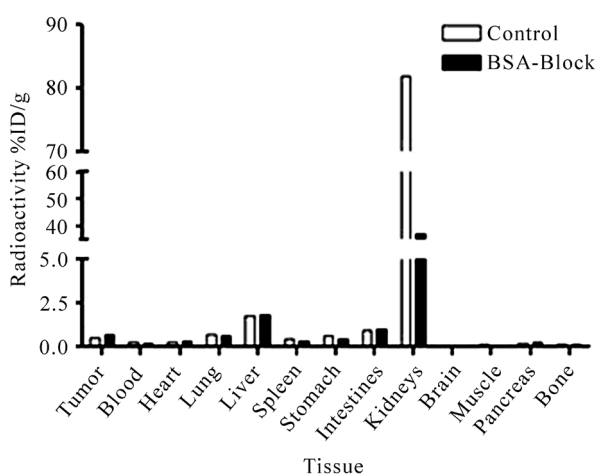
As demonstrated in Figure 5, the tumor uptake and retention of the radiolabeled conjugate was easily visualized in the microPET/CT image and appeared to correlate well with the biodistribution studies observed at 2 h p.i. However, some accumulation of radioactivity was observed in the liver and is in keeping with the biodistribution studies.

Also, substantial radioactivity in the kidneys was clearly evident which correlated well with the biodistribution pattern of the radiolabeled peptide. Since the charge of a peptide can influence renal uptake of a radiolabeled peptide, Sprague et al, suggested that modifica-

tion of the CB-TE2A backbone by addition of a carboxylate arm could improve the distribution kinetics of  $^{64}\text{Cu}$ -CB-TE2A-Y3-TATE by changing the net charge from positive to neutral or negative [22].



(a)



(b)

**Figure 4. Blocking studies with bovine serum albumin fragments, albumin fragments (BSA-F, 200 mg) were preinjected in the mice 5 min prior to the injection of radiolabeled peptides. The kidney uptake of the radioligands in mice with and without BSA-f was measured in a  $\gamma$ -counter. (a) A 43% ( $P = 0.32$ ) and 47% ( $P = 0.037$ ) decrease in the uptake of  $^{64}\text{Cu}$ -DO3A-peptide and (b)  $^{64}\text{Cu}$ -CB-TE2A-peptides was observed, respectively.**

Alternate strategies reported to block the kidney retention of peptides include the use of gelofusine [38], and blocking the uptake by albumin fragments [23]. Our studies with BSA-f indicated a partial kidney block of the radiolabeled peptide *in vivo*. An alternate approach for efficiently blocking the radiolabeled peptide uptake by the kidneys could be to use a combination of BSA-f and the amino acid lysine, simultaneously. Another possibil-

ity would be to replace the amino acid spacers with chemical linkers such as 5-amino-3-oxapentyl-succinamic acid (5-ADS), 8-amino-3,6-dioxaoctyl-succinamic acid (8-AOS), and *p*-aminobenzoic acid (AMBA), between

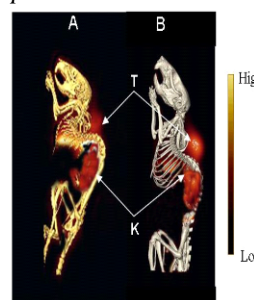


**Figure 5. MicroPET/CT of MDA-MB-435 tumor-bearing mice. A)  $^{64}\text{Cu}$ -DO3A-peptide or B)  $^{64}\text{Cu}$ -CB-TE2A-peptide 12 MBq (324 mCi) was injected into the tail vein of SCID mice bearing MDA-MB-435 tumor xenograft. Imaging was acquired 2 h post injection of the radiolabeled peptides in a PET scanner. The PET images were fused with conventional microCT images to validate regions of increased radiolabeled peptide uptake. Left lateral view images are shown which depicts the distribution of radiolabeled peptides in tumor and other organs. T-tumor, K-kidneys.**

(a)

(b)

**Figure 5. MicroPET/CT of MDA-MB-435 tumor-bearing mice. (a)  $^{64}\text{Cu}$ -DO3A-peptide or (b)  $^{64}\text{Cu}$ -CB-TE2A-peptide 12 MBq (324 mCi) was injected into the tail vein of SCID mice bearing MDA-MB-435 tumor xenograft. Imaging was acquired 2 h post injection of the radiolabeled peptides in a PET scanner. The PET images were fused with conventional microCT images to validate regions of increased radiolabeled peptide uptake. Left lateral view images are shown which depicts the distribution of radiolabeled peptides in tumor and other organs. T-tumor, K-kidneys.**

the bifunctional-chelator and the amino terminus of the peptide, which might influence the kidney clearance of the peptide, as reported previously for bombesin peptide analogs [39]. Overall, our study indicates that the  $^{64}\text{Cu}$ -DO3A- and  $^{64}\text{Cu}$ -CB-TE2A-peptides could be developed into a radioimaging agent for tumors expressing gal-3, and further improvements with respect to the bifunctional chelator or the linkers might improve the  $^{64}\text{Cu}$ -chelate *in vivo* stability and clearance in the circulation.

## 4. Conclusions

$^{64}\text{Cu}$ -DO3A- and  $^{64}\text{Cu}$ -CB-TE2A-(GSG)-G3-C12 were evaluated for MDA-MB-435 breast carcinoma cell binding capacity, *in vivo* biodistribution and microPET imaging of gal-3 expressing breast tumors in heterotransplanted mice. The radiolabeled peptides exhibited specific binding to the carcinoma cells, and targeted the tumors *in vivo* which was clearly demonstrated in microPET imaging. The rapid clearance of the peptides

reduced non-target background except for the liver and kidneys. It remains to be seen whether chelator or spacer modification will further help to improve the renal handling of the radiometallo-peptides.

## 5. Acknowledgements

We thank Dr. Said Figueroa for help with the imaging experiments at the Harry S. Truman Veterans Hospital. We acknowledge Dr. Carolyn Anderson, Washington University School of Medicine, St Louis, for providing the chelator CB-TE2A. The authors also acknowledge Lisa Watkinson and Terry Carmack for performing animal experiments and Marie Dickerson for technical help. This work was supported in part by a Merit Review Award from the Veterans Administration and NIH (P50 CA103130-01).

## 6. References

- [1] S. H. Barondes, D. N. Cooper, M. A. Gitt and H. Leffler, "Galectins: Structure and Function of a Large Family of Animal Lectins," *The Journal of Biological Chemistry*, Vol. 269, No. 33, 1994, pp. 20807-20810.
- [2] S. Sato and R. C. Hughes, "Regulation of Secretion and Surface Expression of Mac-2, a Galactoside Binding Protein of Macrophages," *The Journal of Biological Chemistry*, Vol. 269, No. 6, 1994, pp. 4424-4430.
- [3] I. K. Moutsatsos, M. Wade, M. Schindler and J. L. Wang, "Endogenous Lectins from Cultured Cells: Nuclear Localization of Carbohydrate Binding Protein 35 in Proliferating 3T3 Fibroblasts," *Proceedings of the National Academy of Sciences of the United States*, Vol. 84, No. 18, 1987, pp. 6452-6456. [doi:10.1073/pnas.84.18.6452](https://doi.org/10.1073/pnas.84.18.6452)
- [4] N. L. Perillo, M. E. Marcus and L. G. Baum, "Galectins: Versatile Modulators of Cell Adhesion, Cell Proliferation, and Cell Death," *Journal of Molecular Medicine*, Vol. 76, No. 6, 1998, pp. 402-412. [doi:10.1007/s001090050232](https://doi.org/10.1007/s001090050232)
- [5] S. Sato, I. Burdett and R. C. Hughes, "Secretion of the Baby Hamster Kidney 30-kDA Galactose Binding Lectin from Polarized and Nonpolarized Cells: A Pathway Independent of the Endoplasmic Reticulum-Golgi Complex," *Experimental Cell Research*, Vol. 207, No. 1, 1993, pp. 8-18. [doi:10.1006/excr.1993.1157](https://doi.org/10.1006/excr.1993.1157)
- [6] H. Inohara and A. Raz, "Functional Evidence That Cell Surface Galectin-3 Mediate Homotypic Cell Adhesion," *Cancer Research*, Vol. 55, No. 15, 1995, pp. 3267-3271.
- [7] H. Inohara, S. Akahani, S. Kohts and A. Raz, "Interactions between Galectin-3 and Mac-2-Binding Protein Mediate Cell-Cell Adhesion," *Cancer Research*, Vol. 56, No. 19, 1996, pp. 4530-4534.
- [8] I. Wang, H. Inohara, K. J. Pienta and A. Raz, "Galectin-3 Is a Nuclear Matrix Protein Which Binds RNA," *Biochemical and Biophysical Research Communications*, Vol. 217, No. 1, 1995, pp. 292-303. [doi:10.1006/bbrc.1995.2777](https://doi.org/10.1006/bbrc.1995.2777)
- [9] W. G. Stetler-Stevenson, S. Aznavoorian, L. A. Liotta, "Tumor Cell Interactions with the Extracellular Matrix during Invasion and Metastasis," *Annual Review of Cell Biology*, Vol. 9, No. 1993, pp. 541-573.
- [10] L. A. Liotta, "Cancer Cell Invasion and Metastasis," *Scientific Americana*, Vol. 266, No. 2, 1992, pp. 54-63. [doi:10.1038/scientificamerican0292-54](https://doi.org/10.1038/scientificamerican0292-54)
- [11] V. V. Glinsky, G. V. Glinsky, K. Rittenhouse-Olson, M. E. Huflejt, O. V. Glinskii, S. L. Deutscher and T. P. Quinn, "The Role of Thomsen-Friedenreich Antigen in Adhesion of Human Breast and Prostate Cancer Cells to the Endothelium," *Cancer Research*, Vol. 61, No. 12, 2001, pp. 4851-4857.
- [12] J. E. Lehr and K. J. Pienta, "Preferential Adhesion of Prostate Cancer Cells to a Human Bone Marrow Endothelial Cell Line," *The Journal of the National Cancer Institute*, Vol. 90, No. 2, 1998, pp. 118-123. [doi:10.1093/jnci/90.2.118](https://doi.org/10.1093/jnci/90.2.118)
- [13] P. Nangia-Makker, V. Hogan, Y. Honjo, S. Baccarini, L. Tait, R. Bresalier and A. Raz, "Inhibition of Human Cancer Cell Growth and Metastasis in Nude Mice by Oral Intake of Modified Citrus Pectin," *The Journal of the National Cancer Institute*, Vol. 94, No. 24, 2002, pp. 1854-1862.
- [14] G. V. Glinsky, J. E. Price, V. V. Glinsky, V. V. Mosine, G. Kiriakova and J. B. Metcalf, "Inhibition of Human Breast Cancer Metastasis in Nude Mice by Synthetic Glycoamines," *Cancer Research*, Vol. 56, No. 23, 1996, pp. 5319-5324.
- [15] V. V. Glinsky, G. V. Glinsky, O. V. Glinskii, V. H. Huxley, J. R. Turk, V. V. Mossin, S. L. Deutscher, K. J. Pienta and T. P. Quinn, "Intravascular Metastatic Cancer Cell Homotypic Aggregation at the Sites of Primary Attachment to the Endothelium," *Cancer Research*, Vol. 63, No. 13, 2003, pp. 3805-3811.
- [16] J. Zuo, V. V. Glinsky, L. A. Landon, L. Mathews and S. L. Deutscher, "Peptides Specific to the Galectin-3 Carbohydrate Recognition Domain Inhibit Metastasis-Associated Cancer Cell Adhesion," *Carcinogenesis*, Vol. 26, No. 2, 2005, pp. 309-318.
- [17] S. R. Kumar and S. L. Deutscher, "<sup>111</sup>In-Labeled Galectin-3 Gtargeting Peptide as a SPECT Agent for Imaging Breast Tumors," *Journal of Nuclear Medicine*, Vol. 49, No. 5, 2008, pp. 796-803. [doi:10.2967/jnumed.107.048751](https://doi.org/10.2967/jnumed.107.048751)
- [18] D. J. Rowland, J. S. Lewis and M. J. Welch, "Molecular Imaging: The Application of Small Animal Positron Emission Tomography," *Journal of Cellular Biochemistry*, Vol. 87, No. 39(Supplement), 2002, pp. 110-115. [doi:10.1002/jcb.10417](https://doi.org/10.1002/jcb.10417)
- [19] P. McQuade, Y. Miao, J. Yoo, T. P. Quinn, M. J. Welch and J. S. Lewis, "Imaging of Melanoma Using <sup>64</sup>Cu- and <sup>86</sup>Y-DOTA-ReCCMSH(Arg11), a Cyclized Peptide Analogue of Alpha-MSH," *Journal of Medicinal Chemistry*, Vol. 48, No. 8, 2005, pp. 82985-82992. [doi:10.1021/jm0490282](https://doi.org/10.1021/jm0490282)
- [20] Y. Wu, X. Zhang, Z. Xiong, Z. Cheng, D. R. Fisher, S. Liu, S. S. Gambhir and X. Chen, "MicroPET Imaging of

Glioma Integrin $\alpha$ v $\beta$ 3 Expression Using  $^{64}\text{Cu}$ -Labeled Tetrameric RGD Peptide," *Journal of Nuclear Medicine*, Vol. 46, No. 10, 2005, pp. 1707-1718.

- [21] C. A. Boswell, C. A. Regino, K. E. Baidoo, K. J. Wong, A. Bumb, H. Xu, D. E. Milenic, J. A. Kelley, C. C. Lai, M. W. Brechbiel, "Synthesis of a Cross-Bridged Cyclam Derivative for Peptide Conjugation and  $^{64}\text{Cu}$  Radiolabeling," *Bioconjugate Chemistry*, Vol. 19, No. 7, 2008, pp. 1476-1484. [doi:10.1021/bc800039e](https://doi.org/10.1021/bc800039e)
- [22] J. E. Sprague, Y. Peng, X. Sun, G. R. Weisman, E. H. Wong, S. Achilefu and C. J. Anderson, "Preparation and Biological Evaluation of Copper-64-Labeled Tyr3-octreotate Using a Cross-Bridged Macrocyclic Chelator," *Clinical Cancer Research*, Vol. 10, No. 24, 2004, pp. 8674-8682. [doi:10.1158/1078-0432.CCR-04-1084](https://doi.org/10.1158/1078-0432.CCR-04-1084)
- [23] E. Vegt, J. E. van Eerd, A. Eek, W. J. Oyen, J. F. Wetzels, M. de Jong, F. G. Russel, R. Masereeuw, M. Gotthardt and O. C. Boerman, "Reducing Renal Uptake of Radiolabeled Peptides Using Albumin Fragments," *Journal of Nuclear Medicine*, Vol. 49, No. 9, 2008, pp. 1506-1511. [doi:10.2967/jnumed.108.053249](https://doi.org/10.2967/jnumed.108.053249)
- [24] T. E. Hui, D. R. Fisher, J. A. Kuhn, L. E. Williams, C. Nourigat, C. C. Badger, B. G. Beatty and J. D. Beatty, "A Mouse Model for Calculating Cross-Organ Beta Doses from Yttrium-90-Labeled Immunoconjugates," *Cancer*, Vol. 73, No. 3(Supplement), 1994, pp. 951-957. [doi:10.1002/1097-0142\(19940201\)73:3+<951::AID-CNCR2820731330>3.0.CO;2-1](https://doi.org/10.1002/1097-0142(19940201)73:3+<951::AID-CNCR2820731330>3.0.CO;2-1)
- [25] W. H. Miller, C. Hartmann-Siantar, M. A. Descalle, J. Lehmann, M. R. Lewis, T. Hoffman, J. Smith, P. Situ and W. A. Volkert, "Mouse Organ Absorbed Dose Fractions for Beta Emitters," *Transactions of the American Nuclear Society*, Vol. 89, 2003, pp. 689-692.
- [26] S. R. Kumar, F. A. Gallazi, R. Ferdani, C. J. Anderson, T. P. Quinn and S. L. Deutscher, "In Vitro and In Vivo Evaluation of  $^{64}\text{Cu}$  Radiolabeled KCCYSL Peptides for Targeting Epidermal Growth Factor Receptor-2 in Breast Carcinomas," *Cancer Biother Radiopharm*, Vol. 25, No. 6, 2010, pp. 6693-6703. [doi:10.1089/cbr.2010.0820](https://doi.org/10.1089/cbr.2010.0820)
- [27] J. E. Price, A. Polyzos, R. D. Zhang and L. M. Daniels, "Tumorigenicity and Metastasis of Human Breast Carcinoma Cell Lines in Nude Mice," *Cancer Research*, Vol. 50, No. 3, 1990, pp. 717-721.
- [28] J. M. Rae, S. J. Ramus, M. Waltham, J. E. Armes, I. G. Campbell, R. Clarke, R. J. Barndt, M. D. Johnson, E. W. Thompson, "Common Origins of MDA-MB-435 Cells from Various Sources with Those Shown to Have Melanoma Properties," *Clinical and Experimental Metastasis*, Vol. 21, No. 6, 2004, pp. 543-552. [doi:10.1007/s10585-004-3759-1](https://doi.org/10.1007/s10585-004-3759-1)
- [29] A. F. Chambers, "MDA-MB-435 and M14 Cell Lines: Identical but Not M14 Melanoma?" *Cancer Research*, Vol. 69, No. 13, 2009, pp. 5292-5293. [doi:10.1158/0008-5472.CAN-09-1528](https://doi.org/10.1158/0008-5472.CAN-09-1528)
- [30] C. A. Boswell, X. Sun, W. Niu, G. R. Weisman, E. H. Wong, A. L. Rheingold and C. J. Anderson, "Comparative in Vivo Stability of Copper-64-Labeled Cross-Bridged and Conventional Tetraazamacrocyclic Complexes," *Journal of Medicinal Chemistry*, Vol. 247, No. 6, 2004, pp. 1465-1474. [doi:10.1021/jm030383m](https://doi.org/10.1021/jm030383m)
- [31] L. A. Bass, M. Wang, M. J. Welch and C. J. Anderson, "In Vivo Transchelation of Copper-64 from TETA-Octreotide to Superoxide Dismutase in Rat Liver," *Bioconjugate Chemistry*, Vol. 1, No. 4, 2000, pp. 527-532. [doi:10.1021/bc990167l](https://doi.org/10.1021/bc990167l)
- [32] M. Yu, H. Qing, H. Guojian, Z. Shu, W. Wenqing, H. Youfeng and J. T. Kuikka, "Biodistribution of  $^{64}\text{Cu}$  Cu2+ and Variance of Metallothionein during Tumor Treatment by Copper," *Nuclear Medicine and Biology*, Vol. 25, No. 2, 1998, pp. 111-116. [doi:10.1016/S0969-8051\(97\)00169-8](https://doi.org/10.1016/S0969-8051(97)00169-8)
- [33] D. Ma, F. Lu, T. Overstreet, D. E. Milenic and M. W. Brechbiel, "Novel Chelating Agents for Potential Clinical Applications of Copper," *Nuclear Medicine and Biology*, Vol. 29, No. 1, 2002, pp. 91-105. [doi:10.1016/S0969-8051\(01\)00287-6](https://doi.org/10.1016/S0969-8051(01)00287-6)
- [34] H. Akizawa, Y. Arano, T. Uezono, M. Ono, Y. Fujioka, T. Uehara, A. Yokoyama, K. Akaji, Y. Kiso, M. Koizumi and H. Saji, "Renal Metabolism of  $^{111}\text{In}$ -DTPA-D-Phe<sup>1</sup>-octreotide in Vivo," *Bioconjugate Chemistry*, Vol. 9, No. 6, 1998, pp. 662-670. [doi:10.1021/bc9702258](https://doi.org/10.1021/bc9702258)
- [35] T. M. Jones-Wilson, K. A. Deal, C. J. Anderson, D. W. McCarthy, Z. Kovacs, R. J. Motekaitis, A. D. Sherry, A. E. Martell and M. J. Welch, "The in Vivo Behavior of Per-64-Labeled Azamacrocyclic Complexes," *Nuclear Medicine and Biology*, Vol. 25, No. 6, 1998, pp. 523-530. [doi:10.1016/S0969-8051\(98\)00017-1](https://doi.org/10.1016/S0969-8051(98)00017-1)
- [36] H. Akizawa, Y. Arano, M. Mifune, A. Iwado, Y. Saito, T. Mukai, "Effect of Molecular Charges on Renal Uptake of  $^{111}\text{In}$ -DTPA-conjugated Peptides," *Nuclear Medicine and Biology*, Vol. 28, No. 7, 2001, pp. 761-768. [doi:10.1016/S0969-8051\(01\)00241-4](https://doi.org/10.1016/S0969-8051(01)00241-4)
- [37] B. F. Bernard, E. P. Krenning, W. A. Breeman, E. J. Rolleman, W. H. Bakker, T. J. Visser, H. Mäcke and M. de Jong, "D-lysine Reduction of Indium-111 Octreotide and Yttrium-90 Octreotide Renal Uptake," *Journal of Nuclear Medicine*, Vol. 38, No. 12, 1997, pp. 1929-1933.
- [38] E. Vegt, J. F. Wetzels, F. G. Russel, R. Masereeuw, O. C. Boerman, J. E. van Eerd, F. H. Corstens and W. J. Oyen, "Renal Uptake of Radiolabeled Octreotide in Human Subjects is Efficiently Inhibited by Succinylated Gelatin," *Journal of Nuclear Medicine*, Vol. 47, No. 3, 2006, pp. 432-436.
- [39] J. C. Garrison, T. L. Rold, G. L. Sieckman, F. Naz, S. V. Sublett, S. D. Figueroa, W. A. Volkert and T. J. Hoffman, "Evaluation of the Pharmacokinetic Effects of Various Linking Group Using the  $^{111}\text{In}$ -DOTA-X-BBN(7-14)NH<sub>2</sub> Structural Paradigm in a Prostate Cancer Model," *Bioconjugate Chemistry*, Vol. 19, No. 9, 2008, pp. 1803-1812. [doi:10.1021/bc8001375](https://doi.org/10.1021/bc8001375)